Turkish Journal of Electrical Engineering & Computer Sciences

http://journals.tubitak.gov.tr/elektrik/

Research Article

Turk J Elec Eng & Comp Sci
(2020) 28: 2979 – 2996

doi:10.3906/elk-2004-68

Chronic obstructive pulmonary disease severity analysis using deep learning on multi-channel lung sounds

Gökhan ALTAN*, **Yakup KUTLU**, **Ahmet GÖKÇEN**
Department of Computer Engineering, Faculty of Natural and Engineering Sciences,
İskenderun Technical University, Hatay, Turkey

Received: 09.04.2020 • **Accepted/Published Online:** 05.06.2020 • **Final Version:** 25.09.2020

Abstract: Chronic obstructive pulmonary disease (COPD) is one of the deadliest diseases which cannot be treated but can be kept under control in certain stages. COPD has five severities, including at-risk, mild, moderate, severe, and very severe stages. Diagnosis of COPD at early stages needs additional clinical tests for even experienced specialists. The study aims at detecting the severity of the COPD to start treatment for preventing the progression of the disease to the next levels. We analyzed 12-channel lung sounds with different COPD severities from RespiratoryDatabase@TR. The lung sounds were recorded from the clinical auscultation points from 41 patients on posterior (chest) and anterior (back) sides. 3D second-order difference plot was applied to extract characteristic abnormalities on lung sounds. Cuboid and octant-based quantizations were utilized to extract characteristic abnormalities on chaos plot. Deep extreme learning machines classifier (deep ELM), which is one of the most stable and fast deep learning algorithms, was utilized in the classification stage. Novel HessELM and LuELM autoencoder kernels were adapted to deep ELM and reached higher generalization capabilities with a faster training speed against the conventional ELM autoencoder. The proposed deep ELM model with LuELM autoecoder has separated five COPD severities with classification performance rates of 94.31%, 94.28%, 98.76%, and 0.9659 for overall accuracy, weighted-sensitivity, weighted-specificity, and area under the curve (AUC) value, respectively. The proposed deep analysis of 12-channel lung sounds provides a standardized and entire lung assessment for identification of COPD severity. Our study is a pioneering approach that directly focuses on lung sounds. Novel deep ELM kernels have performed a higher generalization and fast training compared to conventional kernels.

Key words: Deep ELM, RespiratoryDatabase@TR, deep learning, ELM autoencoder, COPD severity

1. Introduction

Auscultation is a physical examination technique that is used to assess the prognoses of internal body organs such as the heart, lungs, and bowel using stethoscopes. Auscultation of the lungs still remains its frequent use for respiratory disorders [1]. Since lung sounds are directly related to structural defects of the lungs, analyzing lung sounds provides more robust and accurate prognoses to identifying abnormalities of the respiratory diseases. The caverns related to the bronchial degeneration and losing elasticity of the patterns in the lung cause pathological respiratory sounds, including wheeze and crackles [2]. Pathological lung sounds occur depending on obstructions, inflammations, and pleural effusion with complete atelectasis in the lungs. Different pathological lung sounds give the specialists hints about various cardiac and pulmonary diseases [3]. Wheeze, which is the most important symptom of COPD, occurs by reason of narrow airways and obstructions arising out of sputum. It is a continuous

*Correspondence: gokhan.altan@iste.edu.tr

pathology with musical clearance in both exhalation and inhalation. Whereas normal lung sound is a quiet and audible in breathing cycle at a frequency range between 100 and 1000 Hz, wheeze is louder and high-pitched due to forced breathing cycle at higher than 400 Hz [4]. The frequency-domain, time-domain, and spectogram plots for a single respiratory cycle are depicted in Figure 1.

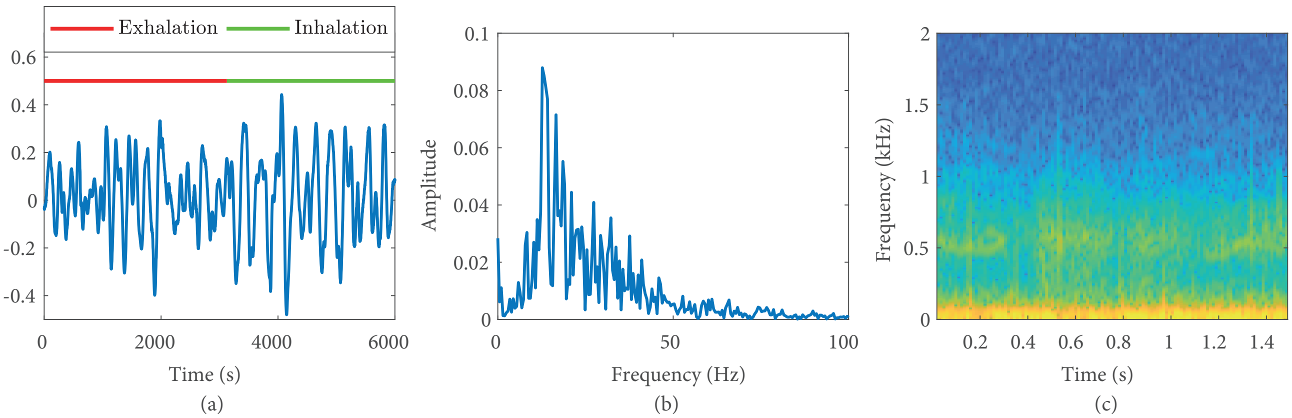

Figure 1. Time-domain (a), frequency-domain (b), and spectogram (c) plots of a single respiratory cycle including inhale and exhale stages on a random patient lung sound auscultation areas at back and chest.

Chronic obstructive pulmonary disease (COPD) is a respiratory disease that has rapid morbidity and mortality across the world. The most important reason for the increasing population of COPD is likely global smoking epidemic in the community for the middle-aged patient population [5]. COPD is a consequence of the limitation on the progressive airflow, the obstructions, and destructions of mainly small airways. Degeneration of the alveoli is why COPD is an incurable and progressive disease [3]. However, COPD can be kept under control and can be managed at a stabilized course through appropriate treatment methods using early diagnosis. Airflow limitations are measured using pulmonary function tests. Forced expiratory volume in 1 s (FEV1) and forced vital capacity (FVC) of the lungs and ratio of FEV1/FVC are used to stage the severities of respiratory diseases [2]. Global Initiative for Chronic Obstructive Lung Disease (GOLD) has categorized the severity of COPD into five classes depending on the wheeze on lung sounds and spirometry airflow limitations of the patients [1, 3]. People who are smokers for a few years are at under risk severity of COPD (COPD0) and have nonchronic symptoms, persistent cough, and an FEV1 ratio higher than 85%. Patients at mild severity of COPD (COPD1) have some chronic symptoms, light wheezing, and an FEV1 ratio higher than 80%. Patients at moderate severity of COPD (COPD2) have most of the chronic symptoms, wheezing, and an FEV1 ratio between 50% and 80%. COPD3 and COPD4 have significant wheezing during expiration and inspiration originated from obstruction and narrowing of airways and commonly concomitant cardiac diseases. The patients at a severe level of COPD (COPD3) have all of the chronic symptoms, prevalent pulmonary infections, and an FEV1 ratio between 30% and 50%. The patients at a very severe level of COPD (COPD4) have all of the chronic symptoms, bedridden case with respiratory machine, and an FEV1 ratio lower than 30% [3]. COPD0-1-2 are hard to diagnose and to identify the characteristics of lung sounds [6].

The lack of research on COPD severity classification has brought about constraints including the analysis of the COPD at early severities, attaining to the COPD1-2, separating COPD1-2 from the smokers, and controlling the progression of COPD convolution [6]. Although lung sound is the most significant and useful diagnostic to detect respiratory diseases, our literature review revealed no lung sound-based COPD severity analysis. Moreover, there are also a limited number of studies on the computerized analysis of COPD, separation of smokers from COPD severities, and abnormality identification in respiratory sounds. Many of these studies focused on the detection of abnormalities in lung sounds and the classification of respiratory sounds. Naves et al. analyzed pathological lung sounds using high-order statistical features (cumulants). They identified computerized crackle and wheeze lung sounds using genetic algorithms on linear and nonlinear classifiers to improve separation performance [7]. Fernandez-Granero et al. utilized the tracheal respiratory sounds to detect early exacerbation of COPD. They extracted discrete wavelet transform-based statistical features from respiratory sounds and proposed a nonlinear model to identify exacerbation [8]. Oweis et al. separated adventitious lung sounds into ten classes using the power spectrum density and morphological features. They proposed an efficient artificial neural network model on the extracted feature set [9]. Additionally, some studies focused on analyzing alternative biomedical signals that are related to breathing activities to predict COPD separation. Kanwade and Bairagi studied instantaneous changes in electromyography (EMG) through breathing. They utilized clinical spirometry measurements, nonfiducial, morphometric, and statistical features from EMG signals. They assessed the chest movements along with breathing and distinguished COPD and non-COPD subjects using support-vector machine classifier [10]. Newandee et al. proposed a method that was based on heart rate variability (HRV) measurements to diagnose COPD. They classified COPD and non-COPD subjects using principal component analysis and clustering algorithms [11]. Altan et al. proposed a nonlinear method to quantize consecutive differences of the data points on lung sounds. They applied the quantization method to separate COPD0 from COPD4 severities for explaining the efficiency of difference plotting on early diagnosis of COPD and classified the COPD severities using the deep belief networks (DBN) classifier [6]. They performed a binary classification which separated two extreme severities (at risk stage and very severe stage of COPD). The focused severities are the easiest to diagnose due to wheeze density in lung sounds. Moreover, their proposal needs additional feature selection stage with greedily DBN classifier which consists of supervised and backpropagation with ANN. The main contributions of this study are analyzing all five severities which are difficult to distinguish without additional spirometry tests even for experienced pulmonologists, performing this analysis by advantages of novel ELM autoencoder proposals by adapting fast learning procedures without iterations to deep models, and excluding feature selection stage by the advantages of autoencoder on generating compressed representations.

Deep learning (DL) has an upward sloping curve in machine learning algorithms. It assumes high detailed classification and low-, high-level feature learning stages using a combination of unsupervised and supervised learning techniques [12]. DL is a two-step classifier that applies unsupervised training at the first step to predefine the model weights and sequentially supervised training to update the predefined weights for obtaining optimum model parameters [13]. The DL consists of effective and robust algorithms including convolutional neural networks (CNN), deep reinforcement learning, DBN, generative autoencoder networks, deep extreme learning machines (deep ELM). Deep ELM, which is one of the fastest and high generalizing capacity algorithms, utilizes ELM autoencoder (ELM-AE) kernels to generate different representations of the input data [14]. Tissera and McDonnell utilized deep ELM to classify images based on character recognition from online databases [15]. Yin and Zhang proposed a deep ELM model to classify electroencephalography signals using various autoencoder kernels [16]. Thang et al. applied deep ELM to normalized and histogram equalized images for face detection, gesture recognition, and car detection [17]. Altan and Kutlu classified Hilbert-Huang transform based features using deep ELM with Hessenberg kernel and performed a brain activity classifier on slow cortical potentials in stroke patients [18]. Khatab et al. proposed a Deep ELM model for solving fingerprint-based indoor localization problems using the autoencoder kernel representation technique on image dataset [19]. Generalization capability and high training speed of the Deep ELM enable enhancing models for detailed analysis of the patterns. Herein, we predicted that these superiorities of the deep ELM could be applied to the classification stages of analysis models.

Early diagnosis of COPD is a matter of vital importance to avoid the progression of the disease and to improve the quality of life for people. Whereas identifying the COPD0-1-2 severities is almost impossible without using additional clinic diagnostics, developing computerized analysis methods on lung sounds provides quick and robust assessments at early stages even without being dependent on expert pulmonologist clinicians [1]. Herein, the paper aimed to classify the severity of COPD using nonlinear quantization techniques and novel DL algorithms. The study focused on extracting 3D-second-order difference plot (3D-SODP) quantization features from multichannel lung sounds and utilizing generalization advantages of deep ELM on the classification stage. The main significances of the paper are analyzing multichannel lung sounds for a general assessment, utilizing Deep ELM advantages for many hidden layers, and separating five of COPD severities using 10 s auscultation scenario. In this analysis, novel ELM autoencoder kernels (lower-upper triangulation ELM and Hessenberg decomposition ELM) were adapted to the deep ELM models. In this manner, the generalization capacity and fast training time of novel ELM autoencoder kernels could be implemented into deep learning algorithms.

In this paper, we present an approach to automatically classify different stages of severity of the COPD using multichannel lung sounds. The key contributions of the proposed system are as follows:

(1) Whereas most studies focus on clinical data to identify COPD severities, for the first time, the identification strategy is applied to estimate five COPD severities using lung sounds considering that lung sounds are the most important diagnostic tool for respiratory diseases.

(2) Rather than relying on using raw lung sounds, this approach depends on 3D-SODP quantization, which efficiently extracts characteristic pathologies; this can effectively reduce input size for time-series.

(3) Novel ELM autoencoder kernels are adapted to deep ELM models to enhance the training capabilities of deep models.

(4) ELM autoencoder kernels are used for feature dimensionality reduction with compressed representation. The efficiency of funnel-shaped deep ELM models is reported. The experimental results in fewer training samples and thereby substantially improved the training efficiency.

The rest of the paper gives detailed information about the database, 3D-SODP, deep ELM classifier, and ELM autoencoder kernel in Section 2. Structure of the proposed deep ELM classifier, iteration parameters, quantization parameters, experimental setup, and achievements are shared in Section 3. The efficiency of deep ELM on COPD severity analysis, superiority, and limited aspects of the proposed models are evaluated in the last section.

2. Materials and method

2.1. Database

In particular, computerized analysis of diseases, which are difficult to detect even if the initial prediagnosis is possible before reaching advanced levels, allows physicians to increase the number of prognoses about patients with COPD. Analyzing lung sounds, which are the biological markers of the respiratory system, enables us to identify respiratory diseases using the most significant characteristics and pathologies.

RespiratoryDatabase@TR is a highly versatile and major premise database, which focuses on chronic and common respiratory disease COPD. It includes 12-channel lung sounds, 4-channel heart sounds, spirometry metrics, and chest X-rays for each subject [20]. RespiratoryDatabase@TR has an ethical committee approval confirmed by Mustafa Kemal University, Turkey (06.03.2015-12). We aimed at identifying the severity of COPD using multichannel lung sounds. Two pulmonologist clinicians auscultated the lung sounds from left (L) and right (R) focus points on the chest and the back using two digital stethoscopes. The auscultation points are depicted in Figure 2. The subjects were labeled using wheeze characteristics of lung sounds, clinical metrics, chest X-ray, and spirometry. Two pulmonologists approved the severity of COPD with common approval on the diagnosis. Many diseases, including congestive heart failure, coronary diseases, diabetes, and tension, accompany COPD3 and COPD4 due to aging reasons and smoking for many years. Therefore, no patient was excluded from the population by reasons of chronic conditions other than lung diseases such as asthma, chronic bronchitis, lower respiratory tract infection, etc. The demographic information, age, sex, and auscultation scenario are detailed in [20].

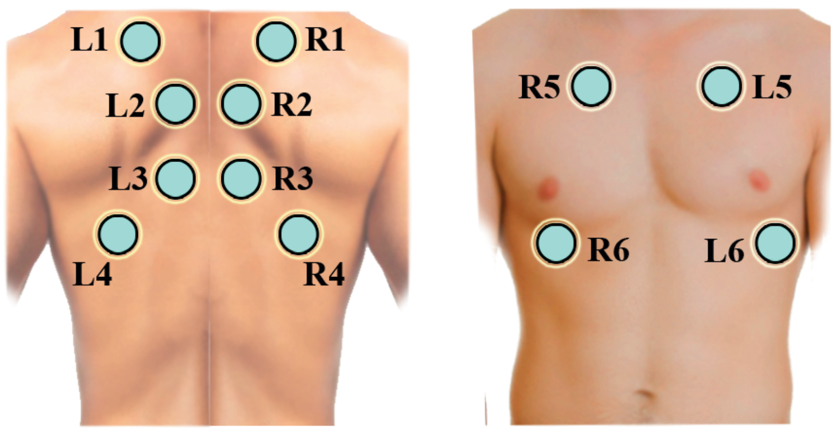

Figure 2. Lung sounds are commonly auscultated from anterior (chest) and posterior (back) sides of the body within a shape of lung anatomy for respiratory diseases. The right (R) and left (L) sides of the auscultation areas in RespiratoryDatabase@TR.

Lung sounds from different auscultation regions have different characteristics depending on the density of the obstructions and thickness of the tissue. Hence, we utilized 12-channel lung sounds from 41 patients with COPD (5 patients with COPD0, 5 patients with COPD1, 7 patients with COPD2, 7 patients with COPD3, and 17 patients with COPD4) in the analysis [1]. Lung sounds were digitized at a sampling frequency of 4000 Hz. The digital stethoscope eliminates ambient noise and patient-based noises with a rate of 85%. Wheeze is a high-pitched continuous sound having frequencies higher than 400 Hz [21].Hence, we did not use a low-pass filter to avoid losing the significant information in the recordings. We applied the Butterworth high-pass filter of 1st order to each lung sound at 7.5 Hz to remove DC offset [6]. We used whitening transformation that changes the input signal into a white noise signal by transforming random variables using declared covariance matrix into identity matrix, before applying 3D-SODP [22].

[1] Mendeley Data (2020). RespiratoryDatabase@TR (COPD severity analysis) [online], Website http://dx.doi.org/10.17632/p9z4h98s6j.1 [accessed 12 June 2020]

2.2. 3D-second-order difference plot

The SODP is a nonlinear method that is commonly used to assess the irregularity of the time series using the difference of the successive data points [23]. Whereas the fixed time series indicates a normal distribution at a specific restrained region, abrupt changes causing pathological conditions have irregular chaos on the SODP [25]. Using the quantization-based features can extract significant characteristics to identify the abnormalities in time series [25]. 3D-SODP is the advanced level of the chaos theory for assessing the location of the data points on space. The 3D-SODP enlarges the analyzing capability of the consecutive data points using an additional difference in time-series. Increasing the dimensional variety on a visualization plot provides a more detailed statistical analysis [6]. SODP provides the opportunity to evaluate the plotted points in a limited area, even if it is pathological. 3D-SODP allows determining the distance of data points to each other distributions using space-based quantization. The 3D-SODP visualizes the decisiveness of regularity [6]. If $lung(n)$ is denoted as the lung sound: the data points for 3D-SODP are calculated using $X(n) = [lung(n+1) - lung(n)]$, $Y(n) = [lung(n+2) - lung(n+1)]$, and $Z(n) = [lung(n+3) - lung(n+2)]$.

The quantization of 3D-SODP is performed by dividing the space into subspaces using various geometric polyhedrons and calculating plotted data points in the subspaces [6]. In this study, we used octant-based and cuboid polyhedrons-based quantizations. The octant-based quantization segments space into eight spaces by three planes such as XY-plane, YZ-plane, and XZ-plane that define signs of the point at abscissa, ordinate, and applicate coordinates (see Figure 3). The cuboid polyhedrons-based quantization segments the spaces into a k-by-k number of subspaces that are centered at the origin with linearly increasing cuboid sizes (see Figure 4).

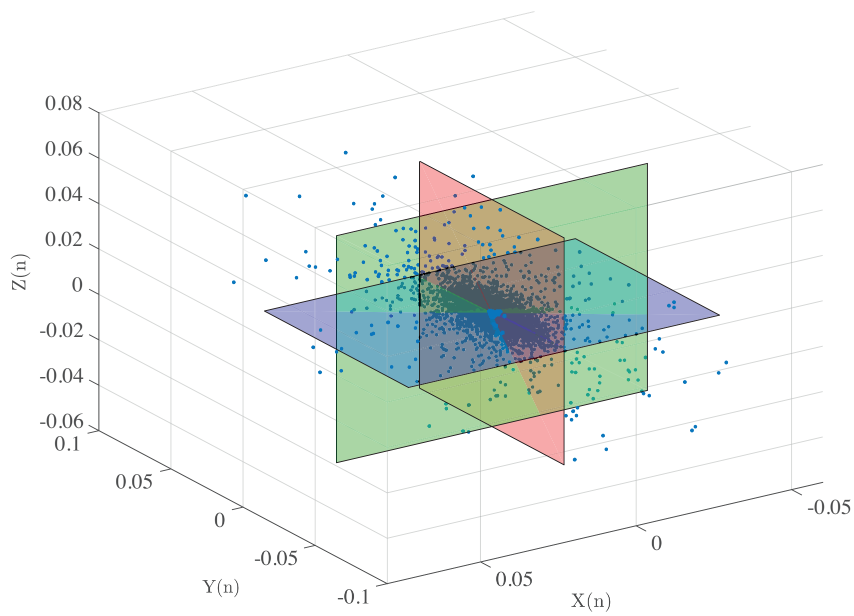

Figure 3. The octant-based quantization of 3D-SODP. The planes intersect at zero. Three planes segment the 3D-SODP space into eight octants (2^3). The signum function defines the concern of the points in 3D-SODP using sign values at each plane.

One of the most critical settings for quantization 3D-SODP is defining the border limits. As a result of this, we used the specific metrics of the SODP. The SODP has an elliptical form in distribution. Therefore, we calculated the major semiaxis (SD_1) of the elliptical form of the SODP for each instance on the dataset.

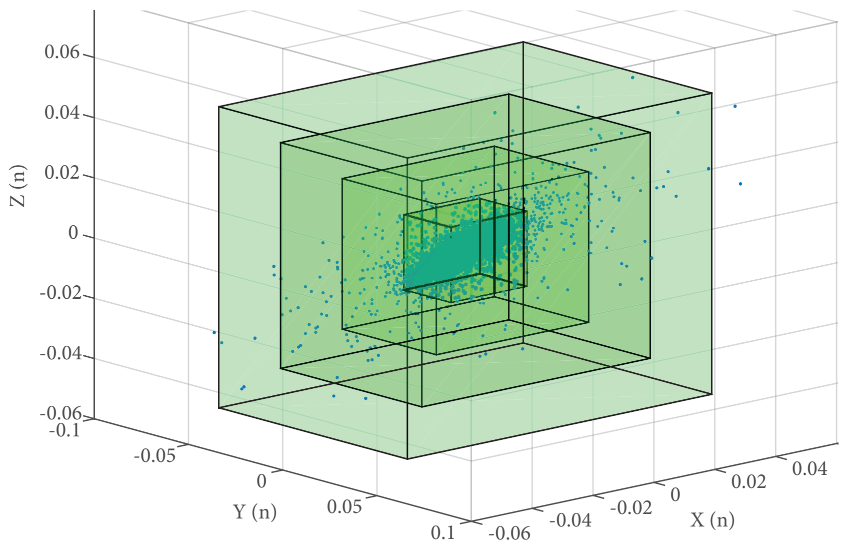

Figure 4. The cuboid polyhedrons-based quantization of 3D-SODP. The 3D-SODP space is segmented into cuboid-polyhedrons that are origin-centered. Each inner cuboid-polyhedron is excluded from the outer cuboid-polyhedrons to obtain nonintersection spaces as feature sets.

The calculation of SD_1 is detailed in [6]. The mean of SD_1 measurements was set as the border to limit the maximum border of the segmentation. The data points out of the limited borders are summed as the outer space feature of 3D-SODP [6].

2.3. Deep extreme learning machines

DL is a trending classifier algorithm that is becoming popular with increasing acceleration in the efficiency of image processing. The most distinctive features of the DL are feature-learning approach and shared weights models. Although the shared weights are used at the learning stages with the emergence of feature learning, the DL model has many parameters that need to be optimized owing to the size of hidden layers of the model and the neurons at each layer [6, 13, 18].

ELM is a single hidden layer feed-forward network (SLFN) model that calculates the output weights of the model (β) using randomly assigned input weights, biases, and hidden node parameters on Moore-Penrose generalized inverse solution [26, 27]. It has a universal approximation validity on generating different presentations using almost any nonlinear mathematical theory [26, 28]. The theory of multilayer ELM is detailed in [17].

Apart from the conventional SLFN ELM models [28], ELM kernels have also been applied to the multilayer deep ELM models. The deep ELM is one of the fastest and most robust classifiers to analyze hierarchical representations. It encodes the input data using various kernel types and various neuron sizes. Deep ELM creates different representations of input data at each layer with preferred output size, including compression, sparse, and equal dimension architecture [19, 25]. The ELM autoencoder (ELM-AE) acts as the feature extractor by generating different presentations of the input data with the same, reduced, and increased sizes [17]. The ELM-AE calculates the output weights (β_i) of i^{th} layer (h_i) by setting T_i as both input and output matrix of the ELM-AE structure.

The encoded final representation of input data was fed into the supervised ELM classifier [15, 17, 25]. Figure 5 depicts the structure of the deep ELM with β transfer representation.

The ELM-AE kernel has different modifications of alternative inverse solutions. Hessenberg decomposition-based ELM-AE (HessELM-AE) is one of the most effective and simplistic encoding kernels [18, 29]. Hessenberg decomposition is an inverse solution that expresses a matrix into a unitary matrix and a tri-diagonal symmetric matrix [30]. Hessenberg matrix (H^+) is solved using $H^+ = H^T(H^T H)^{-1}$ and $H^T H = QUQ^*$, where Q is a unitary matrix, and U stands for the upper Hessenberg matrix. If the equation is replaced, we get $H^+ = H^T (QUQ^*)^{-1}$, and finally $H^+ = H^T QU^{-1}Q^*$ for Hessenberg decomposition.

On the other hand, lower-upper triangulation based ELM-AE (LuELM-AE) is one of the most efficient autoencoder kernels for deep learning models [31]. LuELM-AE decomposes stability inverse once for calculating several matrices for the diagonal matrix. We assume the matrix has upper and lower triangular matrices $H = (LU)$, LuELM-AE calculates $HW = (LU)W = L(UW) = b$, where $UW = d$ and $Ld = b$. L stands for lower triangular matrix, U is the upper triangular matrix in inverse solution. b matrix is solved using forward substitution, and d is solved backward substitution [31].

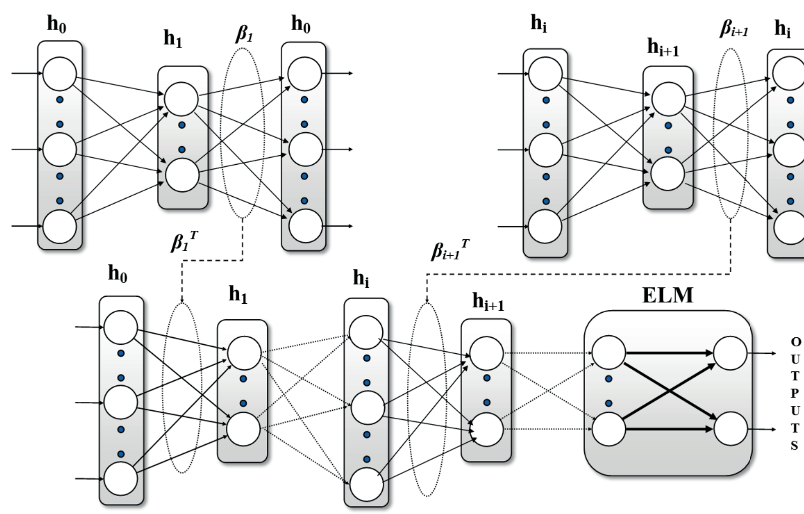

Figure 5. The structure of the deep ELM. Each adjacent pairwise layer establishes an autoencoder model in Deep ELM. The output weight matrix of the autoencoders is transferred as encoding weight matrix to calculate the node weights of the following layer. Whereas the deep AE generates the output weight matrices unsupervised ways, ELM performs supervised learning procedure without iterations at the last layer of the deep ELM.

The ELM-AE model is an unsupervised learning algorithm. Each hidden layer of the deep ELM stands for a different encoding type of the input data. The essential characteristics of the deep ELM are hosting the generalization capability of the ELM, analyzing the various presentations in detailed models, shortening the training time by simplistic solutions, attaining the classification parameters by unsupervised ELM-AE models in the pretraining without iterations.

LuELM and HessELM were adapted to the supervised learning stages with high generalization capabilities of decomposition techniques in [31]. One of the novelties of the work is enhancing LuELM an HessELM kernels to autoencoder kernels for establishing multiple layer models with the advantages of analyzing big data in effective and fast solutions to get higher generalization capabilities for deep learning models. The most significant deficiencies of DL are training speed and excessive dependence on the amount of data. The adaptation of HessELM-AE and LuELM-AE kernels into deep ELM provides a fast training speed and high generalization for even small- and middle-scale dataset. The main superiority of the proposed HessELM-AE and LuELM-AE on ELM-AE is handling pseudoinverse computation drawback using upper triangular decomposition matrix instead of solving whole matrix. To evaluate the main advantages of the proposed deep ELM kernels, we experimented on the same dataset with the same parameters for comparison with conventional ELM-AE and ELM.

3. Experimental results

Short-term and rare pathologies on lung sounds are difficult to detect for even skilled specialists without using detailed physical examination and additional diagnostic tools. Computer-aided analysis of the clinical methods is of great importance for the detection and interpretation of the aforementioned pathologies. Moreover, it is possible to determine the severity of COPD, depending on the duration and intensity of adventitious vibrations. In this regard, minimizing the dependence on skilled clinical specialists and the establishment of prediagnosis systems are the foremost steps to specify the progress and treatment processes of many diseases.

In this study, we used multichannel lung sounds to identify the characteristic pathologies for analyzing the severity of COPD. We extracted 3D-SODP quantization features to assess the dispersion of the signals. Although deep autoencoder kernels have the ability of feature dimensionality reduction on time series, we used an efficient feature extraction method to focus on the characteristic changes which represent pathological abnormality on lung sounds. Otherwise, healthy and pathological gaps on lung sound were encoded together using nonlinear functions. It is hard to follow and to identify the pathological gaps that would affect the clinical usability and acceptance. To examine the efficiency of using multichannel lung sounds on the classification of COPD severities, we conducted experiments on deep ELM. The statistical performance metrics such as accuracy, weighted average sensitivity (W-SEN), and weighted average specificity (W-SPE) were calculated to evaluate the efficiency of the experimented parameters on DL models using Eqs. (1–3) [24, 32]. We calculated test metrics using the BDPV package, that is a script for computing the asymptotic confidence intervals for classification performances in diagnostic tests using R. We compared the achievements of deep ELM with different ELM-AE kernels. Furthermore, we highlighted the advantages of HessELM-AE and LuELM-AE kernels in terms of time complexity and classification performances against conventional ELM-AE.

$$Accuracy = \frac{\sum_{COPD=0}^{4} TP_{COPD}}{Allsubjects} \tag{1}$$

$$W - SEN = \frac{\sum_{COPD=0}^{4} \frac{TP_{COPD}}{(TP_{COPD}+FN_{COPD})} * n_{COPD}}{Allsubjects} \tag{2}$$

$$W - SPE = \frac{\sum_{COPD=0}^{4} \frac{TN_{COPD}}{(TN_{COPD}+FP_{COPD})} * n_{COPD}}{Allsubjects} \tag{3}$$

Each lung sound was segmented into 10-s short-term signals, including at least three respiratory cycles that started with the inspiration. Each short-term signal has 40,000 data points. We applied 3D-SODP to the segmented lung sounds. The 3D-SODP depicted distinctive border dispersion for COPD0 and COPD4. Lung sounds with COPD0 were plotted inlying at loci that are so close to the center of 3D-SODP, whereas lung sounds with COPD4 were plotted at distal loci that are close to extremes of the major axis of 3D-SODP. Especially, the number of division lines and the distance between the two lines are essential for polyhedron-based quantization. Otherwise, it is possible to perform thousands of different segmentation methods at undetermined borders on the 3D-SODP space. The semimajor axis of the SODP was set as the outer borders of the quantization to handle this issue. The limited quantization space is segmented into k-by-k numbers of subregions. Segmentation parameter k ranged in value from 3 to 7 subspaces, experimentally. The outer space of the 3D-SODP, which contained the data points far from the semimajor axis of the SODP, was assigned as the outer-space feature to characterize the abnormal dispersion.

The 3D-SODP space was segmented into subspaces using octants and cuboid polyhedrons methods. The cuboid polyhedrons method extracts the space into k number of nesting cuboids, of which centroids are at the origin of 3D-SODP. The amount of data points in each nesting cuboid space excluding inner cuboids is counted as the feature of the 3D-SODP. The feature set is comprised of 26 cuboid polyhedron quantizations, of which outer spaces are common, and eight octant quantizations from 3D-SODP. Each quantization method was evaluated using deep ELM, separately. Moreover, a combination of all cuboid polyhedron quantization features defined as $Cuboid_{all}$ dataset, and the combination of all quantization features collected as the system dataset were evaluated for identification of severity of COPD using deep ELM.

Ten-fold cross-validation was used to evaluate the performance of the deep ELM using an independent feature set. The number of patients has an unbalanced distribution in the dataset. Nine folds were used to train the models, whereas the remaining fold was used to test the training for avoiding overfitting. Thus, the training and testing of the deep models were performed on separate lung sounds to prevent skewed results from an overfitted model.

The number of hidden layers and neurons at each hidden layer are the tunable parameters to designate an optimal deep ELM classifier model. The ELM-AE, which is preferred as an unsupervised learning algorithm, is the pretraining stage of deep ELM. The proposed stable deep ELM optimization parameters were utilized as $\sigma 1 = \sigma 2 = u = v = 2$ [17]. We tested deep ELM within a limited range of the hidden layer and neuron sizes. The optimum parameters for the highest performance on COPD severity identification were presented for each ELM-AE kernel. The deep model ranged in neuron size at each layer between 100 and 750 units. The deep ELM was modeled with two, three, and four hidden layers. The conventional ELM was tested at a range of neuron size between 10 and 750 units (increasing by 10 units). Table 1 presents the highest classification performances for each dataset.

The highest COPD severity identification performances were achieved with classification rates of 57.72%, 48.50%, and 55.86% for accuracy, W-SEN, and W-SPE, separately by using octant-based quantization features of 3D-SODP on deep ELM with HessELM-AE. The most responsible feature sets are octant-based quantization and $Cuboid_5$ for both ELM-AE kernels and HessELM-AE, respectively. Considering the compose of all cuboid features, $Cuboid_{all}$, the highest COPD severity identification was achieved with an accuracy rate of 79.88% by the deep ELM with LuELM-AE. The combination of the cuboid features has increased the separating capability for both three-autoencoder kernels. The octant-based quantization has achieved better performances than cuboid polyhedron models for deep ELM classifiers among the whole quantizations, even though it has a simple sign analysis of the differences for data points in the space.

Deep autoencoder kernels can reduce the feature dimensionality. A combination of all quantization feature sets was fed into the deep ELM models. The deep ELM with LuELM-AE kernel has separated the five types of COPD severities with performance rates of 94.31%, 94.28%, and 98.76% for accuracy, W-SEN, and W-SPE, respectively. The octant-based quantization and $Cuboid_5$ method have a high responsibility for COPD severity

Table 1. The COPD severity identification performances (%) of the deep ELM model for COPD severity classification on each quantization models.

		$Cuboid_3$	$Cuboid_4$	$Cuboid_5$	$Cuboid_6$	$Cuboid_7$	$Cuboid_{all}$	$Octant$	All
LuELM-AE	Accuracy	27.44	31.91	41.87	38.82	42.68	79.88	53.66	94.31
	W-SEN	25.60	32.40	42.80	36.00	39.60	86.80	55.20	94.28
	W-SPE	27.63	31.02	40.91	38.70	42.37	84.21	52.94	98.76
HessELM-AE	Accuracy	25.61	27.24	46.54	36.99	41.26	74.39	57.72	91.46
	W-SEN	24.40	29.20	43.20	39.60	38.40	79.60	48.80	91.41
	W-SPE	25.59	25.63	46.01	35.47	41.00	76.61	55.86	98.04
ELM-AE	Accuracy	20.33	29.07	29.67	41.67	40.24	67.89	44.51	87.20
	W-SEN	20.80	32.80	32.80	39.20	41.60	58.00	42.40	87.03
	W-SPE	19.51	26.64	27.59	41.31	39.17	64.29	43.97	96.89
ELM	Accuracy	16.87	20.33	21.95	23.17	32.93	60.57	37.40	78.66
	W-SEN	20.40	17.20	18.80	25.20	35.60	53.60	32.40	78.62
	W-SPE	13.85	21.59	23.11	21.43	31.20	58.57	37.87	93.72

identification using deep ELM. The octant-based quantization features and the number of data points at the outer-space feature extract the most remarkable characteristics from lung sounds for deep ELM by considering the whole feature set. Table 2 presents the best three achievements in the identification of severity of COPD for deep ELM autoencoder kernels and simple ELM.

Deep ELM with HessELM-AE kernel has performed the fastest training among three ELM-AE kernels.In accordance with Table 2, the proposed Deep ELM models were trained in 2.11 s, 3.07 s, 4.16 s, and 5.71 s for ELM, HessELM-AE, LuELM-AE, and ELM-AE kernel, respectively. LuELM-AE kernel has the highest generalization capability on the identification of the COPD severities for the proposed Deep ELM models. Table 3 shows the identification achievements. Figure 6 indicates the receiver operating characteristic (ROC) curves for the best Deep ELM and ELM models ELM in the identification of COPD severities. The area under the curve (AUC) values are 0.9659, 0.9168, 0.8217, 0.7995 for LuELM-AE, HessELM-AE, ELM-AE, and ELM, respectively.

The lowest identification accuracy rates were achieved for COPD3 and COPD1, as COPD3 and COPD1 were improperly classified with COPD4 and COPD0, respectively. The highest identification performance was achieved for COPD4 with an accuracy rate of 99.02%. In the view of Table 3, it is clear that COPD3 and COPD4 severities are misidentified to each other for 3D-SODP quantization on multichannel lung sounds using deep ELM models.

4. Discussion

Computerized analysis of the COPD is not sufficiently focused on despite the mortality of the disease across the world. Lung sounds and CT images are the most commonly used diagnostic tools for the identification of the COPD severities. Although clinical research supports the auscultation as the most distinctive diagnostic tool for identification of COPD and most of the respiratory diseases, the majority of computer-assisted analysis has focused on the interpretation of clinical data, different biomedical signals.

Studies commonly focused on various types of data for assessing COPD severity. Table 4 presents related studies on COPD severity analysis considering databases, classifiers, methods, and classification performances.

Table 2. The COPD severity identification performances (%) for the deep ELM with three kernels and ELM.

	Models	Accuracy	W-SEN	W-SPE	Time(s)
LuELM-AE	4 Hidden layers (310-250-100-100 neurons)	94.31	94.28	98.76	4.16
	5 Hidden layers (600-220-160-450-180 neurons)	93.29	93.27	98.47	4.41
	4 Hidden layers (370-390-190-170 neurons)	93.09	93.04	98.30	4.04
HessELM-AE	4 Hidden layers (430-210-180-170 neurons)	91.46	91.41	98.04	3.07
	4 Hidden layers (540-430-270-120 neurons)	91.06	90.98	97.97	2.81
	5 Hidden layers (360-280-240-200-130 neurons)	89.23	89.12	97.42	2.91
ELM-AE	4 Hidden layers (410-300-290-110 neurons)	87.20	87.03	96.89	5.71
	5 Hidden layers (620-380-300-230-190 neurons)	82.32	82.10	95.32	5.13
	4 Hidden layers (110-320-270-500 neurons)	81.50	81.26	94.96	5.38
ELM	640 neurons	78.66	78.62	93.72	2.11
	430 neurons	72.56	72.97	92.20	1.89
	380 neurons	72.15	72.58	91.94	1.27

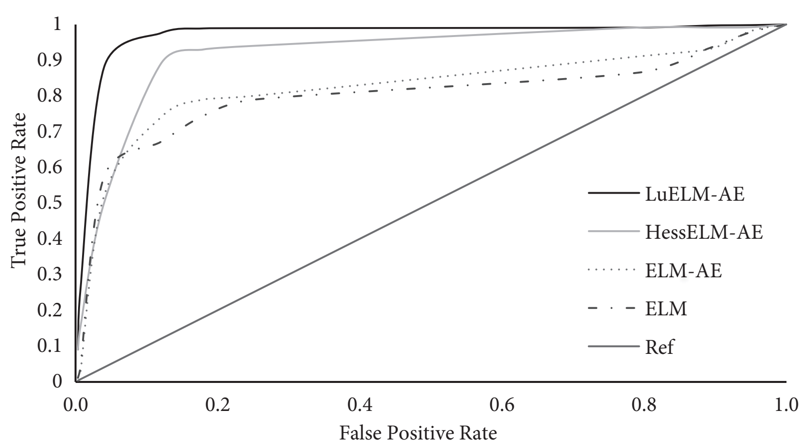

Figure 6. Receiver operating characteristic (ROC) curves of deep ELM and ELM classifiers. AUC value represents the performance of the model in the training. ELM and DeepELM with ELM-AE expose in a similar manner in the training. However, novel ELM-AE and LuELM-AE kernels achieve a better training performance, evidently.

Moghadas-Dastjerdi et al. used image processing techniques on CT images and spirometric test metrics to classify the four COPD severities with an accuracy rate of 84% using Naive Bayes [33]. Though the use of image processing requires much computation power, they achieved a low classification accuracy. Several studies

Table 3. Classification performances (%) for each COPD severity using deep ELM with LuELM-AE kernel.

COPD Severities	Sensitivity	Specificity	Accuracy
COPD0	93.34	99.07	93.33
COPD1	90.01	98.61	90.03
COPD2	93.02	99.01	95.23
COPD3	93.51	97.11	85.71
COPD4	96.65	99.28	99.02

analyzed patient-specific clinical measurements to identify COPD severities. Isik et al. also analyzed clinical data to determine four COPD severities and performed an overall identification performance of 99% using multilayer perceptron [34]. Ying et al. also used clinical data, including symptoms, medical assessment, physical examination, questionnaire answers, and spirometric measurements. They classified the severity of the COPD into five classes with an accuracy rate of 97.2% using DL algorithms [35]. However, spirometric measurements and physical examination assessments can be misleading since their high dependency on the medical device and staff. Whereas some studies directly focused on clinical data, a limited number of them used clinical data as additional features [10, 11]. Kanwade and Bairagi analyzed EMG signals related to chest movements, along with breathing. They received clinical data as additional features. They classified the subjects into COPD and non-COPD with performance rates of 87.80%, 89.65%, and 83.33% for accuracy, sensitivity, and specificity, respectively [10]. However, EMG signals are not suitable for use as a definitive diagnostic tool since they are noisy signals, which are easily affected by normal muscle movements. Newandee et al. utilized HRV, clinical measures, and spectral analysis on ECG. They identified five COPD severities with higher accuracy rates than 88% using principal component analysis and cluster analysis [11]. Whereas HRV measurements are decisive features for cardiac disorders, they act as supportive diagnostics, not a definitive diagnostic tool for respiratory diseases. Furthermore, Newande et al. did not specify how the patients were selected, or whether they used any exclusion criteria related to cardiac status for subjects.

Lung sound still has a very deficient background for computerized analysis of COPD, considering other biomedical signals. A limited number of studies focused on lung sounds for computerized analysis of COPD. Altan et al. applied Hilbert-Huang Transform to 12-channel lung sounds and analyzed the statistical features from frequency-time-domain modulations. They utilized the DBN classifier with different representations using restricted Boltzmann machines. They classified COPD and non-COPD patients instead of COPD severity with performance rates of 93.67%, 91%, and 96.33% for accuracy, sensitivity, and specificity, respectively [13]. Their proposal consists of time-consuming two-step transformation stage with frequency-time-energy distribution analysis comparing to 3D-SODP with simple chaos theory. Morillo et al. focused on extracting fiducial features on tracheal respiratory sounds instead of clinical data. They obtained frequency features, entropy features, and statistical features from respiratory sounds and fed into the artificial neural network classifier to identify two of COPD severities. They achieved classification performance rates of 72.00%, 81.80%, and 77.60% for sensitivity, specificity, and accuracy, respectively [5]. Although it is the closest paper to the proposed model, tracheal respiratory sounds are better at capturing dominant wheeze sounds, which are symptoms of most of the chronic respiratory disease. The most important deficiency of the study is analyzing single-channel tracheal respiratory sounds to assess lung disease. The proposed deep ELM model has an analysis capability on 12-channel lung sounds for a complete lung assessment.

Table 4. Comparison of the related studies on COPD severity analysis.

	Database	Methods	Classifier	Accuray	W-SEN	W-SPE
Sanchez-Morillo et al. [5]	Tracheal sound	STFT	ANN+PCA	77.60	72.00	81.80
Altan et al. [6]	Lung sounds	3D-SODP	DBN+SFS	95.85	93.34	93.65
Newandee et al. [11]	HRV	PCA	Clustering	>88.00	-	-
Moghadas-Dastjerdi et al. [33]	CT images	Image Features	Naïve Bayes	84.18	82.64	-
Ying et al. [35]	Clinical data	-	DBN	97.20	-	-
This study	Lung sounds	3D-SODP	Deep ELM	94.31	94.28	98.76

** STFT: Short time Fourier transform, PCA: Principal component analysis, ANN: Artificial neural network, SFS: Sequential feature selection

The structure of the 3D-SODP presents an elliptical polyhedron. The extreme borders of the dispersion have varied for different COPD severities. The outermost space for the cuboid polyhedron method is significant for the identification of COPD severities. Figure 7 depicts the highly responsible amount of the subspaces for $Cuboid_5$ quantization method.

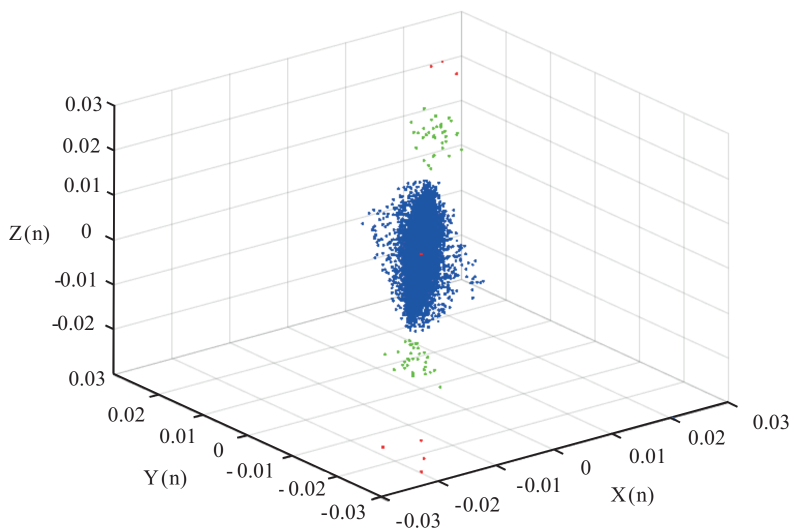

Figure 7. Highly responsible features using $Cuboid_5$ polyhedrons-based 3D-SODP quantization for identification of COPD severities.The red data points are in the outermost space of 3D-SODP. The dispersion of pathological lung sounds occurs an accretion in the outermost, correspondingly impairment in other cuboid-polyhedrons. The severity of the COPD is represented by the outermost and inner spaces.

5. Conclusion

Generally, clinicians are not much interested in model accuracy and other machine learning performance measures, but they need to know how a model decides to assign the COPD state to one of the severity classes. The most responsible octant spaces include the extreme segments of the elliptical polyhedron for 3D-SODP quantization. The achievements prove that quantization of extreme spaces major axis at 3D-SODP, which exhibit sudden changes on the lung sounds, is important to designate the alternate severity of COPD for even lung sounds that have highly similar pathological wheezing to each other. Analysis of 3D-SODP enables the classification of five types of COPD severity by applying the proposed nonlinear quantization algorithm with deep ELM classifiers. The deep ELM classifier with HessELM-AE and LuELM-AE kernels performed an accurate performance of the iterated ranges of classification parameters. Simple ELM had low classification performance against deep ELM models. That is why deep learning has superiority on single layer feed-forward neural networks with using multiple hidden layers. The depth of the model provided more detailed analyzing capability and significant representations of the input for COPD severity analysis.

Detailing segmentation of 3D-SODP by increasing segmentation parameter k ($Cuboid_6$, $Cuboid_7$) has decreased the COPD severity identification performance for deep ELM classifiers. Therefore, increasing the segmentation number k was halted after $Cuboid_7$. It was concluded that the detailed analysis using segmentation with a large number of k results in losing the significance and characteristic of chaos on 3D-SODP. It is important to designate the limit of segmentation distance as preprocessing of the 3D-SODP quantization. The fact that one of the most responsible features is the outer-space feature proves the efficiency of setting the major-axis of the elliptical form as the limit of the segmentation. It has provided to obtain distinctive pathology characteristics for lung sounds on the identification of severity of COPD.

Composing each dataset increases the feature dimensionality in the dataset. Whereas a large dataset enables a detailed analysis of the COPD severities, it may result in overfitting for machine learning algorithms. The quantization of 3D-SODP may contain pointless subspaces for the identification of COPD severities. Hereby, we simply used deep autoencoder kernels to generate compressed representation instead of an additional feature selection algorithm on the identification of COPD severities. Deep ELM kernels generate different presentations of the data at each layer. Therefore, it takes advantage of flexibility on sparsity and compression between layers to eliminate redundant features. It is experienced that the highest classification performances were achieved using the funnel-shaped model on deep ELM by generating sparse representation at the first layer and compressed presentation for remaining ones. j is the feature set dimensionality, k, m, and t denote the number of nodes at 1^{st}, 2^{nd}, and 3^{rd} hidden layer, respectively. The funnel-shaped deep ELM model was set as $j = 34, j < k$ and $k > m > t$.

Deep ELM reduces the feature dimensionality using a compressed representation of autoencoder kernels to avoid the curse of dimensionality. The simple concepts/theories of ELM provide an advantage to ELM-AE kernels for predefinition of classification parameters on the deep ELM models using transfer learning. That is why deep ELM is fast and stable for also detailed classifier models. It makes it possible to use many hidden layers and neurons by feature learning and using shared weights in training. In accordance with the average training time of the best three achievements, the proposed deep ELM models were trained in 1.76 s, 2.93 s, 4.2 s, and 5.4 s for ELM, HessELM-AE, LuELM-AE, and ELM-AE kernel, respectively. The average training times are remarkably accomplished, considering the number of hidden layers and neurons at each layer for deep models. The fastest Deep ELM kernel is HessELM-AE. It is 1.44x and 1.84x faster than LuELM-AE and ELM-AE using CPU, respectively. Whereas training time is a curse for deep learning algorithms, reducing time is one of the most important steps for machine learning algorithms. The deep ELM kernels have high generalization capability as well as high-speed training for deep models and a low number of the subject population.

COPD3 and COPD1 are the most misidentified severities to each other for even best deep ELM models. It is because of the highly similar wheeze pathologies, which are difficult to detect at COPD4 and COPD0 severities respectively for even pulmonologist specialists without additional diagnostics. COPD3 was misclassified as

COPD4. The nonposterior severities could be separated from each other with high-performance rates. The proposed deep ELM models have achieved classification performance rates of 94.31%, 94.28%, and 98.76% for accuracy, W-SEN, and W-SPE on 3D-SODP quantization features of multichannel lung sounds.

The main superiority of this study is estimating the severity of COPD using multichannel lung sounds. It is a pioneering approach that focuses on analyzing multichannel lung sounds for a complete obstruction assessment on the lungs. The study precisely has the advantages of 3D-SODP by extracting quantization of pathological distributions and the deep ELM by possessing detailed and enhanced validity on the representation of many hidden layers.

The small number of subjects constitutes the weakness of the study. It is particularly challenging to diagnose because the symptoms at COPD0-1-2 severities are confused with issues associated with general smoking. Twelve-channel lung sounds, that are from the posterior and anterior points which are standard for a physical examination of COPD, were used for each patient in the analysis to enlarge the number of signals that stand for the severity of COPD. In this way, the subject population was increased by $12\times$. Increasing the number of the auscultation points is more important than synchronization recording. The pathological lung sounds may occur in different parts of the lungs. Hence, using more channels with both simultaneous and synchronous recording may provide a more detailed analysis capability for whole lungs to detect pathological sounds that vary demanding on respiratory diseases. Moreover, experimental results show that the use of the deep ELM reduces the dependence of deep learning algorithms on the number of samples. Therefore, sparse representation on autoencoder ensures generating different presentations of the input data; on the other hand, it performs data augmentation at the first layer.

Acknowledgment

This study was supported by the Scientific and Technological Research Council of Turkey (TÜBİTAK) (TUBITAK-116E190). The authors express their thanks to TÜBİTAK for providing full support.

References

[1] Celli BR, MacNee W, Agusti A, Anzueto A, Berg B et al. Standards for the diagnosis and treatment of patients with COPD: A summary of the ATS/ERS position paper. European Respiratory Journal 2004; 23: 932-946. doi: 10.1183/09031936.04.00014304

[2] Gunen H, Hacievliyagil SS, Yetkin O, Gulbas G, Mutlu LC et al. Prevalence of COPD: First epidemiological study of a large region in Turkey. European Journal of Internal Medicine 2008; 19(7): 499-504. doi: 10.1016/j.ejim.2007.06.028

[3] Roisin RR. Chronic obstructive pulmonary disease updated 2010 global initiative for chronic obstructive lung disease. Global Initiative for Chronic Obstructive Lung Disease 2016; 1: 1-94. doi: 10.1097/00008483-200207000-00004

[4] Meslier N, Charbonneau G, Racineux JL. Wheezes. European Respiratory Journal 1995: 8(11): 1942-8. doi: 10.1183/09031936.95.08111942

[5] Sanchez-Morillo D, Leon Jimenez A, Moreno SA. Computer-aided diagnosis of pneumonia in patients with chronic obstructive pulmonary disease. Journal of the American Medical Informatics Association 2013; 20.e1: 111-117. doi: 10.1136/amiajnl-2012-001171

[6] Altan G, Kutlu Y, Pekmezci AO, Nural S. Deep learning with 3D-second order difference plot on respiratory sounds. Biomedical Signal Processing and Control 2018; 45: 58-69. doi: 10.1016/j.bspc.2018.05.014

[7] Naves R, Barbosa BHG, Ferreira DD. Classification of lung sounds using higher-order statistics: A divide-and-conquer approach. Computer Methods and Programs in Biomedicine 2016; 129: 12-20. doi: 10.1016/j.cmpb.2016.02.013

[8] Fernandez-Granero MA, Sanchez-Morillo D, Leon-Jimenez A. An artificial intelligence approach to early predict symptom-based exacerbations of COPD. Biotechnology and Biotechnological Equipment 2018; 32(3): 778-784. doi: 10.1080/13102818.2018.1437568

[9] Oweis R, Abdulhay E, Khayal A, Awad A. An alternative respiratory sounds classification system utilizing artificial neural networks. Biomedical Journal 2014; 38(2): 153-161. doi: 10.4103/2319-4170.137773

[10] Kanwade A, Bairagi V. Classification of COPD and normal lung airways using feature extraction of electromyographic signals. Journal of King Saud University-Computer and Information Sciences 2019; 31(4): 506-513. doi: 10.1016/j.jksuci.2017.05.006

[11] Newandee DA, Reisman SS, Bartels AN, De Meersman RE. COPD severity classification using principal component and cluster analysis on HRV parameters. In: Proceedings of the IEEE Annual Northeast Bioengineering Conference; Newark, NJ, USA; 2003. pp. 134-135. doi: 10.1109/NEBC.2003.1216028

[12] Hooda R, Mittal A, Sofat S. Lung segmentation in chest radiographs using fully convolutional networks. Turkish Journal of Electrical Engineering & Computer Sciences 2019: 27: 710-722. doi: 10.3906/elk-1710-157

[13] Altan G, Kutlu Y, Allahverdi N. Deep learning on computerized analysis of chronic obstructive pulmonary disease. IEEE Journal of Biomedical and Health Informatics 2020; 24(5): 1344-1350. doi: 10.1109/JBHI.2019.2931395

[14] Yu W, Zhuang F, He Q, Shi Z. Learning deep representations via extreme learning machines. Neurocomputing 2015; 149-Part A: 308-315. doi: 10.1016/j.neucom.2014.03.077

[15] Tissera MD, McDonnell MD. Deep extreme learning machines: supervised autoencoding architecture for classification. Neurocomputing 2016; 174-Part A: 42-49. doi: 10.1016/j.neucom.2015.03.110

[16] Yin Z, Zhang J. Task-generic mental fatigue recognition based on neurophysiological signals and dynamical deep extreme learning machine. Neurocomputing 2018; 283: 266-281. doi: 10.1016/j.neucom.2017.12.062

[17] Tang J, Deng C, Huang GB. Extreme learning machine for multilayer perceptron. IEEE Transactions on Neural Networks and Learning Systems 2016; 27: 809-821. doi: 10.1109/TNNLS.2015.2424995

[18] Altan G, Kutlu Y. Hessenberg Elm Autoencoder Kernel for deep learning. Journal of Engineering Technology and Applied Sciences 2018; 3(2): 141-151. doi: 10.30931/jetas.450252

[19] Khatab ZE, Hajihoseini A, Ghorashi SA. A fingerprint method for indoor localization using autoencoder based deep extreme learning machine. IEEE Sensors Letters 2018; 2: 1-4. doi: 10.1109/LSENS.2017.2787651

[20] Altan G, Kutlu Y, Garbi Y, Pekmezci AO, Nural S. Multimedia respiratory database (RespiratoryDatabase@TR): Auscultation sounds and chest x-rays. Natural and Engineering Sciences 2017; 2: 59-72. doi: 10.28978/nesciences.349282

[21] Vannuccini L, Earis JE, Helisto P, Cheetham BMG, Rossi M et al. Capturing and preprocessing of respiratory sounds. European Respiratory Review 2000; 10(77): 616-620.

[22] Koivunen AC, Kostinski AB. The feasibility of data whitening to improve performance of weather radar. Journal of Applied Meteorology 1999: 38(6): 741-749, doi: 10.1175/1520-0450(1999)038<0741:TFODWT>2.0.CO;2

[23] Pachori RB, Patidar S. Epileptic seizure classification in EEG signals using second-order difference plot of intrinsic mode functions. Computer Methods and Programs in Biomedicine 2014; 113(2): 494-502 doi: 10.1016/j.cmpb.2013.11.014

[24] Altan G, Kutlu Y, Yeniad M. ECG based human identification using second order difference plots. Computer Methods and Programs in Biomedicine 2019; 170: 81-93. doi: 10.1016/j.cmpb.2019.01.010

[25] Song G, Dai Q. A novel double deep ELMs ensemble system for time series forecasting. Knowledge-Based Systems 2017; 134: 31-49. doi: 10.1016/j.knosys.2017.07.014

[26] Huang GB, Zhu QY, Siew CK. Extreme learning machine: Theory and applications. Neurocomputing 2006; 70: 489-501. doi: 10.1016/j.neucom.2005.12.126

[27] Sevinc E, Dokeroglu T. A novel hybrid teaching-learning-based optimization algorithm for the classification of data by using extreme learning machines. Turkish Journal of Electrical Engineering & Computer Sciences 2019: 27(2): 1523-1533. doi: 10.3906/elk-1802-40

[28] Shebab MA, Kahraman N. Optimum, projected, and regularized extreme learning machine methods with singular value decomposition and L 2 -Tikhonov regularization. Turkish Journal of Electrical Engineering & Computer Sciences 2018; 26: 1685-1697. doi: 10.3906/elk-1706-60

[29] Altan G, Kutlu Y. Generative autoencoder kernels on deep learning for brain activity analysis. Natural and Engineering Sciences 2018: 3(3): 311-322. doi: 10.28978/nesciences.468978

[30] Golub GH, Van Loan CF. The Hessenberg and Real Schur Forms, 7.4. In: Golub GH, Loan CFV (editors). Matrix Computations, 3rd ed. Baltimore: Johns Hopkins University, 1996, pp. 1-20.

[31] Kutlu Y, Yayik A, Yildirim E, Yildirim S. LU triangularization extreme learning machine in EEG cognitive task classification. Neural Computing and Applications 2019; 31(4): 1117-1126. doi: 10.1007/s00521-017-3142-1

[32] Isler Y, Narin A, Ozer M, Perc M. Multi-stage classification of congestive heart failure based on short-term heart rate variability. Chaos, Solitons & Fractals 2019; 118: 145–151. doi: 10.1016/j.chaos.2018.11.020

[33] Moghadas-Dastjerdi H, Ahmadzadeh M, Karami E, Karami M, Samani A. Lung CT image based automatic technique for COPD GOLD stage assessment. Expert Systems with Applications 2017; 85: 194-203. doi: 10.1016/j.eswa.2017.05.036

[34] Isik U, Guven A, Buyukoglan H. Chronic obstructive pulmonary disease classification with artificial neural networks. In: 2015 Medical Technologies National Conference (TIPTEKNO); Muğla, Turkey; 2015. pp 1–4. (in Turkish with an abstract in English) doi:10.1109/TIPTEKNO.2015.7374589

[35] Ying J, Dutta J, Guo N, Xia L, Sitek A et al. Gold classification of COPDGene cohort based on deep learning. In: ICASSP, IEEE International Conference on Acoustics, Speech and Signal Processing - Proceedings; Shanghai, China; 2016. pp. 2474-2478. doi: 10.1109/ICASSP.2016.7472122